

Performance Improvement through the Vane Clocking Effect in a Two–Stage Impulse Turbine

Antoni SMOLNY
Jarosław BŁASZCZAK
Krzysztof SOB CZAK
*Institute of Turbomachinery
Technical University of Łódź*

Received (17 August 2011)
Revised (23 September 2011)
Accepted (28 September 2011)

The paper describes the experimental and numerical investigations of stator clocking effects on performance of a two–stage impulse turbine with low–aspect ratio airfoils. The data present the clocking effect that can be observed both for local flow patterns and external characteristics for the entire turbine in terms of efficiency. Finding an optimal relative circumferential position of stators in a multistage axial turbine has been the subject of extensive investigations in the last decade.

Keywords: Impulse turbine, efficiency, clocking, unsteady flow, calculation

1. Introduction

Different relative circumferential positions of stator rows in a two–stage turbine have an influence on the flow behavior in terms of loss generation. Minimization of loss generation in multistage turbomachinery is a key to improve efficiency and, therefore, to increase energy sustainability, to reduce fuel consumption and greenhouse gases and waste production.

A number of experimental and numerical studies have been carried out in recent years to investigate clocking phenomena [2, 3, 4, 7, 10]. Aside of off–design problems [2, 5] a special interest is observed in highly–loaded blade phenomena [1, 8], an influence of the flow unsteadiness on loss generation [7, 9] and the wake boundary layer interactions [1, 2, 11].

Lately, great attention has been drawn to interactions between blade rows, which are especially relevant for the high pressure (HP) turbine design with relatively small aspect ratios, where the secondary flow losses contribute significantly to the reduction of stage efficiency [5, 7, 8, 9, 10].

The clocking effect affects the interaction of the wakes, the end–wall secondary

flow vortices and the unsteady pressure flow field from upstream airfoils with downstream airfoils. It is commonly found that the maximum in the efficiency value could be observed when the wake of an upstream stator hits the leading edge of the subsequent stator. If the wake passes between two stator blades, degradation in efficiency occurs [2]. In a low aspect ratio blade, a three-dimensional flow field is dominated by secondary flow structures. The associated flow effect that originates in the complex unsteady interaction of the wakes, the secondary flow vortices and the blade geometry, contribute to changes in generation and redistribution of the unsteady loss [7, 9, 14].

Detailed steady and unsteady flow measurements and understanding of the flow physics is thus a key requirement in achieving further improvements of turbine efficiency [1–16]. Some of the clocking researchers showed promising results, for example Jouini et al. [8] obtained efficiency variations with 4% peak-to-peak difference. Huber et al. [7] conducted an investigation of different vane clocking positions in a two-stage test turbine with a low aspect ratio profile and found 0.8% efficiency changes versus stator clocking. Generally, the time averaged stage efficiency is a function of the airfoil clocking position.

This paper concerns experimental investigations of the clocking effects on the performance and the flow of the model two-stage impulse turbine and it should give a wider point of view on the clocking phenomena in the complex 3D flow within blade rows.

The experimental work presented herein has been a continuation of the earlier studies, starting from mid-nineties, performed at the Institute of Turbomachinery (Technical University of Lodz, Poland) after modernization the two-stage low-pressure turbine test rig [11–16].

The results of precise measurements of the power and torque output differed with respect to the stator-to-stator clocking position. For the off-design highly loaded turbine conditions, the indexing airfoil phenomena were observed very well and the differences were significant. The relative efficiency changes were about 0.8%. To develop knowledge of the clocking phenomena, the present turbine geometry was designed as for an impulse two-stage turbine, more closely related to the high pressure axial flow steam turbine.

2. Facility and instrumentation

The series of tests were conducted on the two-stage impulse turbine with an eddy-current brake. The turbine with an eddy-current brake (Fig. 1) was situated in the special anechoic chamber enabling to perform also various aeroacoustic studies [5].

The turbine shaft has been connected through a flexible coupling with one end of the Horiba WT190 eddy current dynamometer equipped with a precision torque meter, the maximum torque is 600 Nm and the accuracy 1 Nm. The dynamometer is controlled by a Horiba -Schenck digital 16 bit STARS Lite automation system. Figure 1 shows a schematic layout of the turbine test rig. A three-fan set with a specially equipped control system provided continuous and strictly constant airflow pressure to the test rig (Fig. 2).

Fig. 3 shows the turbine geometry. The vane profiles have been the same for both stators. The airfoil count for the impulse turbine is 22 for the first and second stator.

The rotors designs are characterized by the high turning angle. They are unshrouded disks and have the same blade count of 23 blades. The stators and the rotors incorporate fully cylindrical profiles. The rotors are manufactured as bladed discs (blisks) out of one piece of metal. The manufacturing process ensures an accuracy of the profile shape of 0.05 mm. The stator vanes are attached to the stator cylinder, which gives an opportunity of individual instrumentation of single stator vanes. The turbine design allows the entire stator and rotor rows to be simply disassembled when replacing vane or blade rows for additional instrumentation or another turbine investigations.

As an important part of the safety chain, vibrations of the shaft are measured with acceleration sensors. The signals are processed and displayed by a Sensor vibration diagnostic module.

Special clocking mechanisms were designed to allow the first stage stator to be moved circumferentially with respect to the second stage stator independently of the casing. This allows changing the clocking positions of the first and second stator vanes during the tests without stopping the turbine and dismantling it. The rotors were fixed at the same design relative position without changing it during the tests [16].

Main parameters of "TM3-20" 2-stage axial turbine test rig:

Rotor nominal speed [RPM] 3600

Pressure ratio 1.30

Mass flow [kg/s] 3.50

Blades 22/33

Aspect ratio 1.2/1.5

Tip diameter [mm] 514

Mach number at the rotor exit/stator exit 0.1/0.3

Reynolds number based on the axial chord $2 \cdot 10^5$

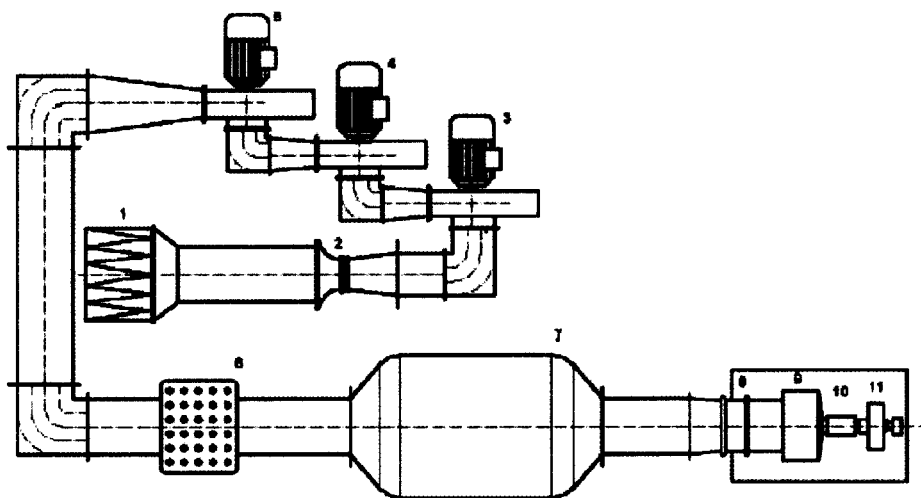


Figure 1 Schematic view of the TM-3 turbine test rig. Outer part: 1 – Air filter; 2 – Venturi contraction; 3 – Fan 1; 4 – Fan 2; 4 – Fan 3; 6 – Cooler; 7 – Stabilizing container; Anechoic room part: 8 – Inlet ring; 9 – Turbine; 10 – Shaft; 11 – Eddy-current brake

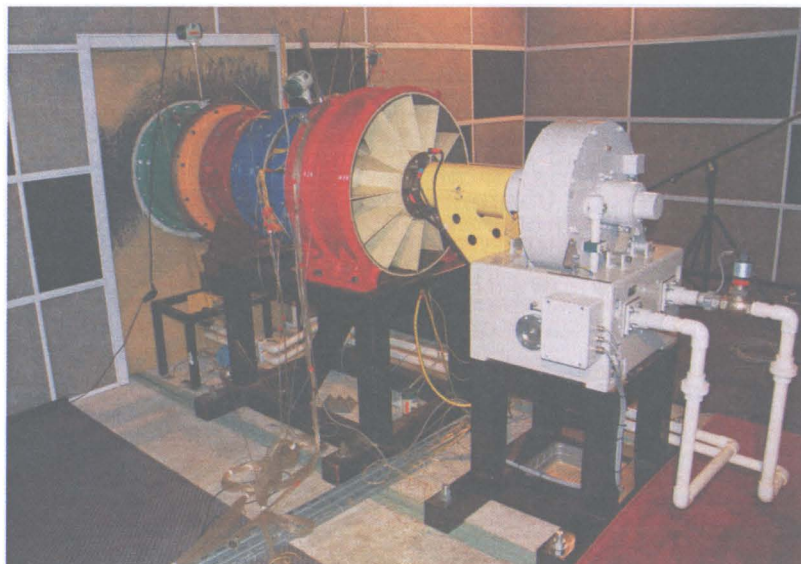


Figure 2 Two-stage axial turbine test rig

During the turbine performance tests, experimental data were obtained for clocking positions of the two stators ranging for the 1.8 relative vane pitch. In some cases (the most time consuming ones) the airfoil indexing was limited only to one pitch range.

For performance measurements, combined total pressure and total temperature rake type probes are used upstream of the first stator row and downstream of the second rotor row. The total pressure probes are the Kiel – Pitot tube types, total temperature probes are calibrated J-type thermocouples. Additionally, at both turbine inlet and exit, PT100 resistance thermometers measure the air temperature [16].

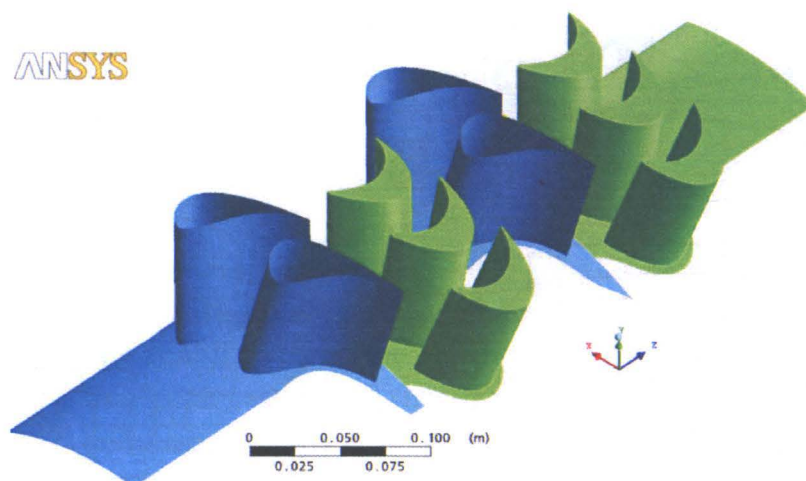


Figure 3 Two-stage impulse turbine configuration. Simulation performed for 2 passages of the stators and 3 passages of the rotors (pitch ratio 1:1)

One humidity sensor is positioned at the exit of the turbine. The Venturi pressure drop is measured with a calibrated Rosemount differential pressure gauge of the

range of 4 kPa (accuracy of 0.04%). The same kind of sensor measure the difference to the atmospheric pressure. The atmospheric pressure is measured with a 0.1 MPa Druck absolute pressure sensor (accuracy of 1 Pa).

Two 16-channel difference-pressure Scanivalve DSA modules measured the pressure distributions on the vanes surfaces.

It is worth noting that the clocking effect influenced the whole test rig, not only the turbine. In earlier studies [11–15] the changes of overall mass flow, inlet flow parameters, etc., were also observed due to the flow clocking effect. In this study special precautions were taken to ensure the constancy of the overall characteristics of the turbine at each operating point, special attention was drawn to the constant rotational speed condition and the difference between the inlet total pressure and the outlet static pressure. The inlet constant pressure was strictly under control during every test session.

During the tests the rotational speed n was constant. The variation of the speed n at the working point was less than 2 rpm during every measurement session due to the brake control system. The inlet air parameters for the tests presented herein were as follows: total pressure (compared to the ambient pressure) $-p_{t0} = 29.860 + / - 0.005$ kPa, total temperature $T_{t0} = 320 + / - 0.2$ K.

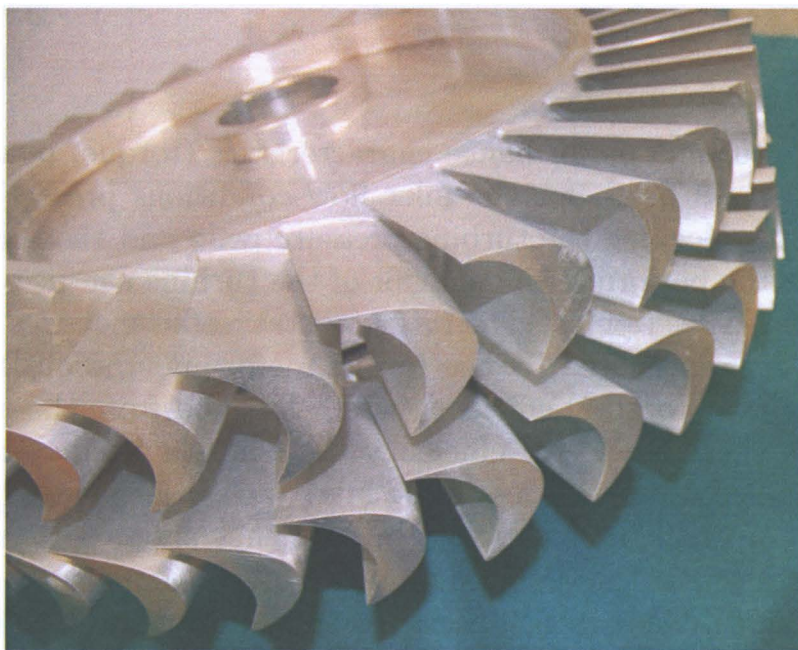


Figure 4 Rotors are manufactured as bladed discs (blisks) out of one piece

During all tests the initial conditions, mainly the inlet and outlet pressures, were controlled all the time to be strictly the same. The data presented in this paper were obtained at the design speed ($n_{nom} = n_1 = 3600$ rpm) and for two off-design rotational speeds ($n_2 = 3060$ rpm and $n_3 = 4140$ rpm).

The major component of the turbine test rig were chosen such that the turbine efficiency accuracy requirements of less than 0.5 % were satisfied [16].

3. Numerical simulation

The three-dimensional, steady-state and unsteady, Reynolds-averaged, compressible Navier-Stokes equations were solved with the ANSYS CFX 12.1 computational code. Multiple numerical analyses of the flow field inside turbomachinery were performed at the Institute of Turbomachinery TUL with this code, e.g., as described by Chodkiewicz et al. [6]. A structured multi-block grid system was generated with the ANSYS TurboGrid software. High quality meshes were obtained. However, due to limitation of the computation time in the case of the unsteady simulations, their refinement this in the boundary region was not sufficient to fully solve the boundary layer and the wall function was used. This approach seems satisfactory because no wall separation was observed.

In the previous computations the Shear Stress Transport *SST* model with an automatic wall function produced the best agreement with the experiments and was adopted as the standard model for the analysis of all turbomachinery complex flows [5, 6, 12]. The preliminary numerical tests performed for this turbine confirmed this choice. At the inlet and the outlet the boundary conditions specified in the previous chapter were applied. The blade, hub and tip wall regions were assumed as adiabatic and the non-slip condition was applied. All the numerical simulations were performed for the design rotational speed. In the case of the stationary simulations the Frozen Rotor interface between stationary and rotational domains was applied.

4. Turbine performance

The two-stage turbine performance characteristics (torque, power, total-to-static efficiency, and mass flow), for the inlet flow conditions presented above, are presented in Fig. 5. Keeping the turbine pressure ratio and the turbine inlet temperature constant the performance behavior of the turbine can be obtained within the chosen rotational speed range. The total-to-static efficiency was obtained using the net turbine power measured by the torque meter and the outlet static (ambient) pressure. The total-to-total efficiency was calculated from the outlet turbine total pressure. The thermodynamic efficiency method was used to calculate efficiency from pressures and temperatures at the inlet and outlet planes of the turbine.

A comparison with the total-to-total efficiency shows systematic discrepancies in measurements with the rotational speed. The difference in levels is probably due to an unknown bias error in the particularly thermodynamic performance calculation method. The calculated total-to-total efficiency from steady simulations agrees very well with thermodynamic efficiency. Steady numerical approaches approximate the real flow in turbines, but they neglect some aspects of real physics. Therefore, it estimates the loss of the unsteady flow in an approximate way. Also as illustrated by computation of the mass flow (Fig. 5), the steady approach, quite popular in the industrial use, can calculate the turbine parameter with the same errors in magnitudes.

To insure the test repeatability, three final efficiency tests were run. Here it is noted that these three tests showed very small discrepancy and they are almost ideally aligned to the single curve.

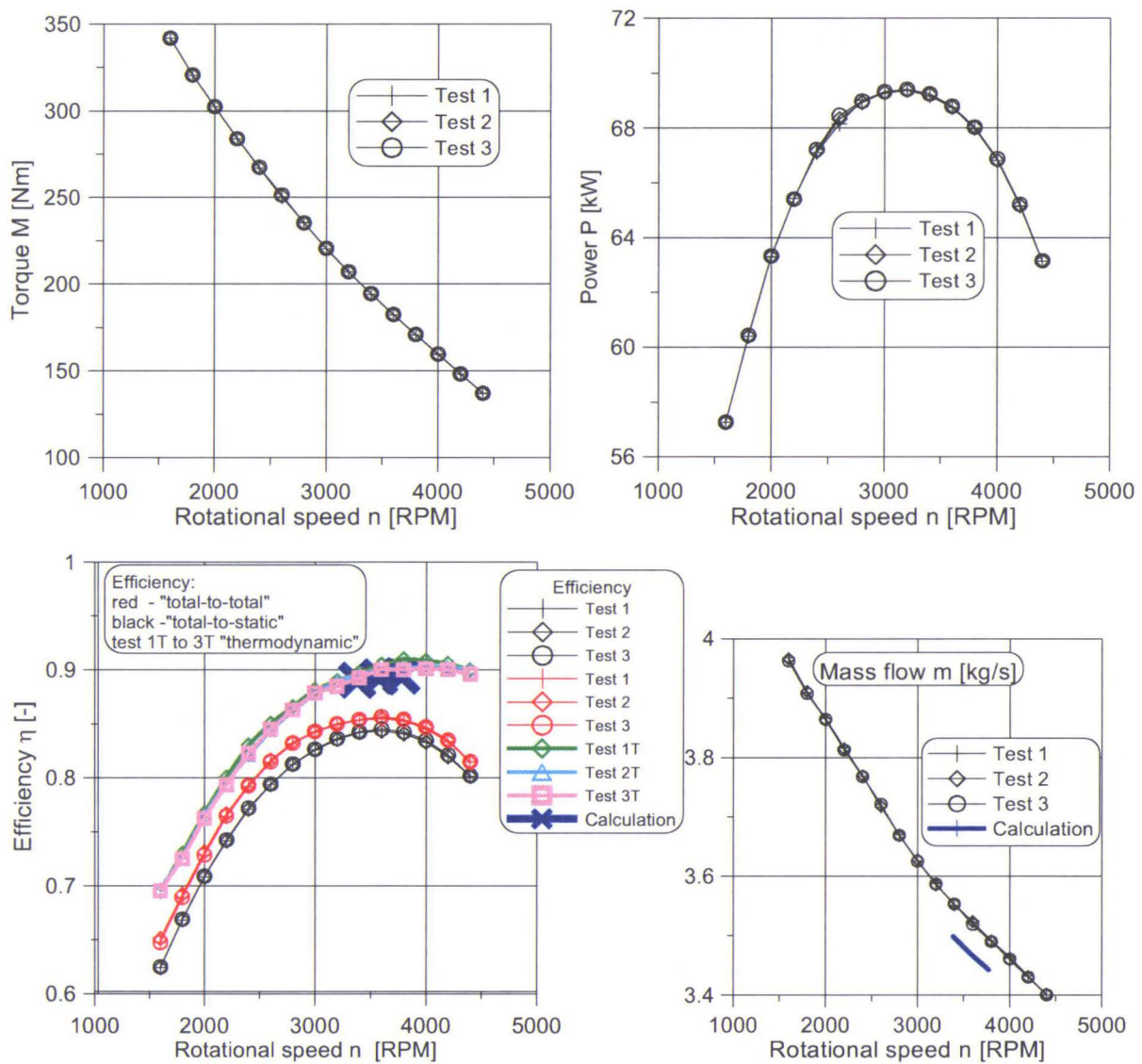


Figure 5 Torque, power, efficiency, and mass flow of the turbine (the experimental results and the numerical steady flow calculations)

5. Analysis of the numerical and experimental results

To give a deeper insight into the physical mechanisms associated with the airfoil clocking, the CFD simulation of real turbine flows can be realized using time dependent numerical methods. However, unsteady computations of the turbine for equal pitches (2 stator and 3 rotor blades) led to an enormous effort and to time-consuming simulations. Therefore, at this moment, calculations were performed only for the nominal rotational speed and one clocking position.

The unsteady entropy distributions at mid-span are shown in Fig. 6. The graphs show the resultant entropy distribution for one stator- rotor position at the $x'/T = 0$ clocking position. Entropy distributions illustrate the wake trajectories in the flow passage. The stator 1 wake is well visible as it interacts with the rotor and the boundary layer. The stator wake is stretched and distorted. However, due to an interaction of the wakes with upstream wakes, it is difficult to identify the origin of each wake.

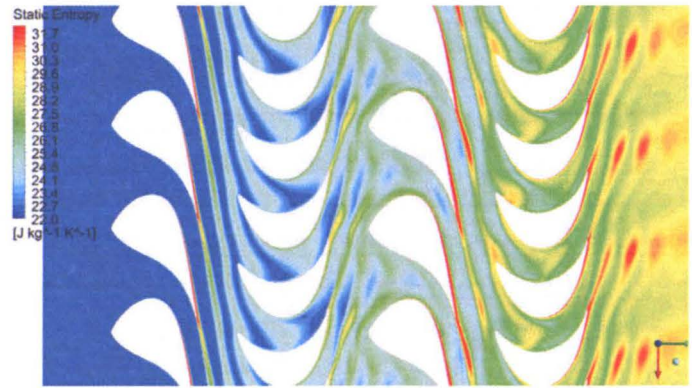


Figure 6 Entropy distribution in unsteady calculations at mid-span

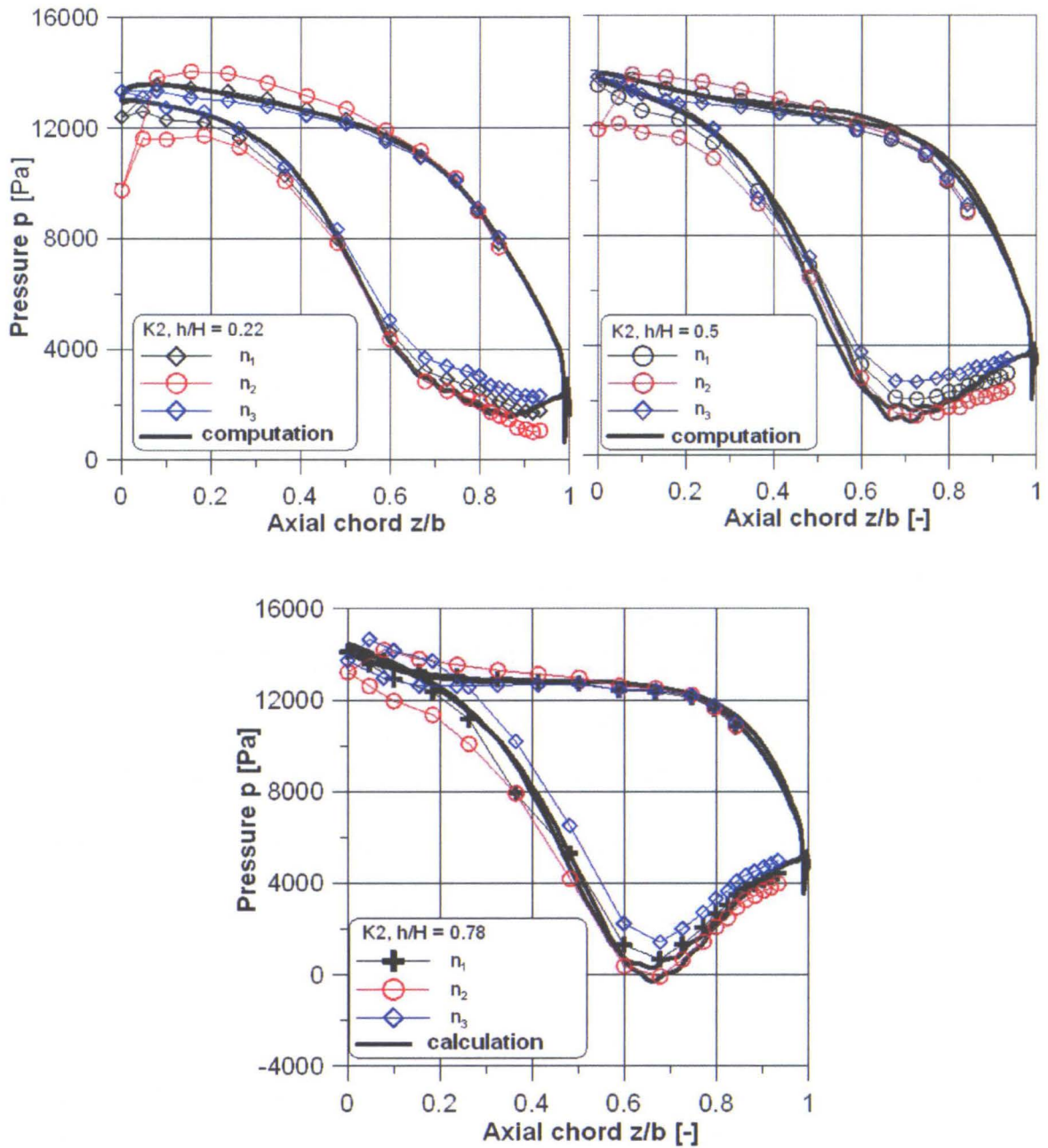


Figure 7 Time averaged surface pressure distribution on the second stator

If we compare the entropy distribution in Fig. 6 at the same stator–rotor relative position, it is obvious that the stator clocking may cause different entropy distributions and the turbine can reach different efficiencies.

Figure 7 shows some experimental results and numerical predictions of the pressure distribution on the second vane surface for three rotational speeds (nominal n_1 and off–design n_2, n_3). In this figure is presented the average surface pressure distribution near the hub, at midspan and the near casing. A good agreement between the measured average pressure (nominal speed n_1) and the time averaged pressure from unsteady calculations is found in general. Further investigations will show if the surface pressure can be a valid representation of a change in performance of the second stator due to clocking in the complex three–dimensional flow field. It was found that the highest efficiencies appeared when the time-averaged surface pressure on the second stator was the highest [2,10].

6. Stator clocking investigations

The results shown in Fig. 8 illustrate the efficiency variation obtained by the first stator clocking with respect to the second stator for the nominal rotational speed. Measurement of the overall performance was acquired for the stator clocking configuration to every 6 % of the stator pitch from the base clocking configuration $x'/T=0$.

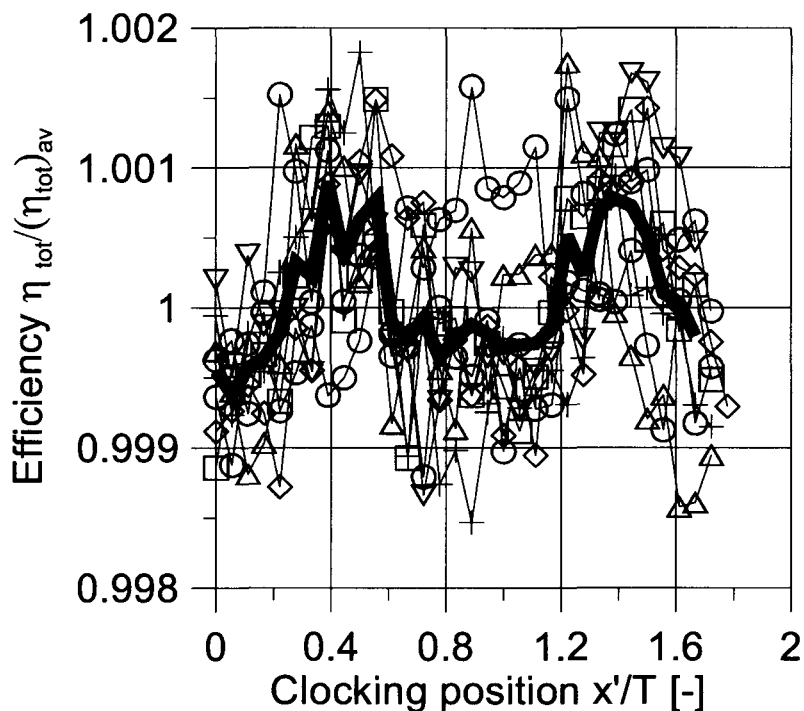


Figure 8 Efficiency of the turbine versus the clocking position

The measurements of the efficiency versus clocking were repeated 7 times. In order to show the tendency more clearly, the relative efficiency distributions were presented in Fig. 8. It can be observed that the particular distributions of the relative efficiency have a similar tendency. Therefore, for each stator clocking position, the measurements were averaged over all 7 trials to obtain distributions of the averaged efficiency as a function of the stator clocking position. It is visible from Fig. 8 that the average efficiency (red) is repeatable the over stator pitch. On the basis of the average distribution of efficiency the maximum variation of efficiency versus clocking is 0.15 % of the mean efficiency. These results are within the accuracy band of the efficiency. However, due to periodic a character of changes, it can be concluded that this approach, proposed by Barankiewicz [3], has an ability to predict the clocking effect.

The test presented in Fig. 8 shows that the clocking effect influencing the turbine performance was found smaller than for the case of the earlier turbine geometry. The reason could be that the local span-wise efficiency variation with the first vane clocking could be out of phase in the radial direction

7. Conclusions

A two-stage impulse turbine with a new geometrical design was prepared for experimental investigations of stator-to-stator clocking effect. Facility is prepared for accurate measurements of the efficiency and performance of the entire turbine.

However, in high-pressure turbines with low aspect ratio profiles, the flow field characteristics may be much different. In this kind of turbine stages, secondary flow vortices can influence the major portion of the span. They can be most important contribution to the variation of performances with clocking.

Pure wake structures are rather of minor importance in the flow field. Therefore the previously described wake model will not be able to cover sufficiently the flow mechanisms, which influence the performance of high-pressure, highly loaded turbines.

Consequently, the future investigations are aimed at an identification of governing flow mechanisms related to the clocking in high-pressure turbines with a highly three-dimensional flow. The secondary flow interaction within the first stage and its effect on the performance and, particularly on the flow field and the performance of the second stator with respect to stator clocking will be analyzed. Fortunately, this complex flow interaction may be correctly predicted by unsteady CFD method. Future numerical investigation and flow measurements will show if a better efficiency improvement can be achieved.

Acknowledgements

The authors would like to thank the research team at the Institute of Turbomachinery TU Lodz for the support in setting up the test facility and help during the extensive research program. The financial supporting has been granted by the Polish State Committee for Scientific Research, Project NN 513427733

References

- [1] **Howell, R.J., Ramesh, O.N., Hodson, H.P., Harvey, N.W. and Schulte, V.:** High Lift and Aft-Loaded Profiles for Low-Pressure Turbines, *ASME, J. Turbomachinery*, 123, pp. 181–188, **2001**.
- [2] **Arnone, A., Bonaiuti, D, Focacci, A., Pacciani. R., Del Greco, A. S. and Spano, E.:** Parametric Optimization of a High-Lift Turbine Vane, *GT2004-54308*, **2004**.
- [3] **Barankiewicz, W.S. and Hathaway, M.D.:** Effects of stator indexing on performance In low Speer multistage Arial compressor, *NASA TM 113113*, **1997**.
- [4] **Behr T., Porreca L., Mokulys T., Kalfas A.I. and Abhari R.S.:** Multistage Aspects and Unsteady Effects of Stator and Rotor Clocking In an Axial Turbine with Low Aspect Ratio Blading, *ASME, GT2004-53612*, **2004**.
- [5] **Błaszczak J.:** Efficiency improvement and noise redukcjon through statot-stator clocking effect of two-stage turbine, *ASME, GT2005-68833*, **2005**.
- [6] **Chodkiewicz R., Sobczak K., Papierski A. and Borzęcki T.:** CFD Code – A usefull tool for the turbomachinery designer, *Task Quarterly* 6, no 4, pp. 553–575, **2002**.
- [7] **Huber, F.W., Johnson, P.D., Sharma, O.P., Staubach, J.B. and Gaddis, S.W.:** Performance Improvement Through Indexing of Turbine Airfoils: Part 1 - Experimental Investigation, *ASME, J. of Turbomachinery*, 118, pp. 630–635, **1996**.
- [8] **Jouini, D.B.M., Little, D., Bancalari, E., Dunn, M., Haldeman, C. and Johnson, P.D.:** Experimental Investigation of Airfoil Clocking Impacts on Aerodynamic Performance in a Two Stage Turbine Test Rig, *ASME, GT2003-38872*, **2003**.
- [9] **Gadea, J., Denos, R., Paniagua G., Billiard N. and Sieverding C.H.:** Effect of Clocking on the Second Stator Pressure Field of a One and a Half Stage Transonic Turbine, *ASME, GT2004-53463*, **2004**.
- [10] **Haldeman, C.W., Dunn M.G., Barter, J.W., Green, B., R. and Bergholz, R.F.:** Experimental Investigation of a Vane Clocking in a One and Stage High Pressure Turbine, *ASME, GT2004-53477*, **2004**.
- [11] **Smolny, A. and Błaszczak, J.R.:** Experimental Investigations Of Unsteady Flow Fields In A Two-Stage Turbine, *2nd EuroConf. on Turbomachinery*, Antwerp, Belgium, **1997**.
- [12] **Sobczak K., Smolny A. and Błaszczak J.:** Quasi-unsteady simulations of clocking phenomena In the two-stage turbine, *Mechanics and Mechanical Eng.*, Vol. 12, No. 2, pp.111–124, **2008**.
- [13] **Krysiński, J., Smolny, A., Błaszczak, J. and Gallus,H.E.:** 3D Unsteady Flow Experimental Investigations in a Two-Stage LP Turbine, *ISUAAAT'2000*, Lyon, France, pp. 515–523, **2000**.
- [14] **Krysiński, J., Błaszczak, J.R. and Smolny, A.:** Stator Clocking Effect on Efficiency of a Two-Stage Low-Pressure Model Turbine, *4th EuroConference on Turbomachinery*, ATI-CST090/01, pp. 1045–1051, Florence, Italy, **2001**.
- [15] **Krysiński, J.E., Błaszczak, J. and Smolny, A.:** Two-stage turbine experimental investigations of unsteady stator-stator interaction, *ISUAAAT'2003*, Durham, NC, **2003**.
- [16] **Krysiński J. Smolny, A., Błaszczak, J. and Sobczak K.:** Badania akcyjnych wieńców łopatek przy wysokich obciążeniach na powietrznej dwustopniowej turbinie modelowej, *Sprawozdanie z projektu NN 513427733 KBN*, **2011**.

Nomenclature

- b – chord [m]
- h – radial coordinate starting from the hub [m]
- H – height of the flow channel [m]
- K1, K2 – the first and the second stator, respectively
- m – mass flow [kg/s]
- M – torque [Nm]
- n – rotational speed [rpm]
- p – pressure [Pa]
- T – temperature [K], vane pitch [m]
- x – circumferential direction
- x'/T – stator-to-stator relative clocking position [-]
- y – radial direction
- z – axial direction